THE JOURNAL OF PHYSICAL CHEMISTRY B

ARTICLE

pubs.acs.org/JPCB

Investigation on the Solubility of SO_2 and CO_2 in Imidazolium-Based Ionic Liquids Using NPT Monte Carlo Simulation

Ahmadreza. F. Ghobadi,[†] Vahid Taghikhani,[‡] and J. Richard Elliott[†,*]

[†]Chemical and Biomolecular Engineering Department, University of Akron, Akron, Ohio 44325, United States

[‡]Department of Chemical and Petroleum Engineering, Sharif University of Technology, Tehran, Iran

ABSTRACT: The solubility of sulfur dioxide (SO_2) and carbon dioxide (CO_2) at P = 1 bar in a series of imidazolium-based room-temperature ionic liquids (RTILs) is calculated by Monte Carlo simulation in NPT ensemble using the OPLS-UA force field and Widom particle insertion method. The studied ILs were 1-butyl-3-methylimidazolium ([bmim]$^+$) tetrafluoroborate ([BF_4]$^-$), [bmim]$^+$ hexafluorophosphate ([PF_6]$^-$), [bmim]$^+$ bromide ([Br]$^-$), [bmim]$^+$ nitrate ([NO_3]$^-$), [bmim]$^+$ bis-(trifluoromethyl) sulfonylimide ([Tf2N]$^-$), and 1-ethyl-3-methylimidazolium tetrafluoroborate ([emim][BF_4]). To validate the simulations, the liquid density of studied ILs and the solubility of CO_2 in [bmim][PF_6] was compared with corresponding experimental and theoretical studies reported in the literature, and a good agreement was obtained. The results of SO_2 solubility demonstrate that the SO_2 gas has the highest solubility in [bmim][NO_3] and [bmim][Br] ILs and the lowest solubility in [bmim][PF_6]. To describe the solubility order of polar gases such as SO_2 and nonpolar gases like CO_2, we have simulated the SO_2/IL and CO_2/IL mixtures which made possible to investigate the interaction of solute molecules with anions and cations in the liquid phase. We introduced the ratio of solute−IL interaction over cation−anion interaction energy density as an index for solubility of gases in ILs. The results show that the proposed index can describe the solubility order of SO_2 as well as CO_2 and it might be used as an alternative to standard methods of infinite dilution Henry's constant calculations when the solubility order is desired.

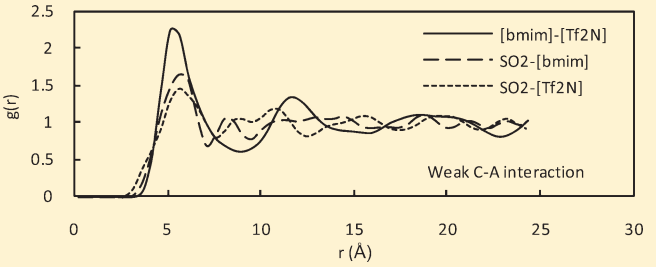

1. INTRODUCTION

Ionic liquids (ILs) are ionic compounds composed entirely of ionic species. ILs have, at least, an ion with a bulky, asymmetric, and organic structure which is a cation in most cases. This structure hinders them from crystallization and leads to their unusual melting temperature. Room-temperature ILs (RTILs) are those that have a melting point below 100 °C.[1,2] The most important property of ILs is their negligible vapor pressure at ambient temperature.[3] Consequently, they are odorless, nonvolatile, and mainly nonflammable, which make them safer and more environmentally friendly than volatile organic compounds.[1,4] As a result of these characteristics, they are called "green" solvents. In addition, it is estimated that with different combinations of cations and anions, countless ILs with varying physical and chemical properties can be produced. Thus, one can tune the properties of ionic liquids by modifying the nature of the anions and cations.

In the past decade, numerous researches were focused on prospective applications of ILs such as solvents of chemical reactions,[5,6] electrochemistry,[7] media for catalyzed or biocatalyzed reactions,[8−10] purification and separation processes,[11] and extraction of desired compounds from gas or liquid phases.[11−14] Many applications of ILs are concerned with dissolution of gases, and for design of such processes, it would be necessary to know solubility of gases in ILs. Two of these gases with a rising significance are SO_2 and CO_2. Combustion of fossil fuels could result in the formation of SO_2 and CO_2, which can lead to acid rain and global warming. Designing suitable processes for separation and removal of these components before atmospheric release of flue gases is crucial. One of the most promising approaches for achieving this goal is selective absorption of undesired gas into a liquid.[15,16] Although there are some commercial processes for flue gas desulfurization,[17] their disadvantages such as low efficiency and huge amount of gypsum waste[18] have inspired many research groups to substitute them with more effective processes. In doing so, ILs seem to have a high potential for selective absorption of SO_2 and CO_2.[19−26]

In the past few years, several theoretical and experimental studies addressed the solubility of different types of gases including SO_2 and CO_2 in RTILs. But, there are controversies over the reasons that describe the solubility order of these gases in ILs. Blanchard et al.[27] measured the solubility of CO_2 in some ILs and presented the solubility order: 1-octyl-3-methylimidazolium hexafluorophosphate ([C_8mim][PF_6]) > 1-butyl-3-methylimidazolium hexafluorophosphate ([bmim][PF_6]) > 1-octyl-3-methylimidazolium tetrafluoroborate ([C_8mim][BF_4]) > 1-butyl-3-methylimidazolium nitrate ([bmim][NO_3]). They concluded that there is a direct relation between IL molar volume and the solubility of CO_2. In other words, higher molar volume of IL can result in

Received: May 31, 2011
Revised: September 5, 2011
Published: September 28, 2011

higher solubility of CO_2. Anthony et al.[28] measured the solubility of water in three ILs and observed the following solubility order: $[C_8mim][BF_4] > [bmim][PF_6] > [C_8mim][PF_6]$. They mentioned that smaller anions provide more room for solute to locate in the liquid phase. Also, smaller ions have more charge density resulting in greater interaction between ions and solute. So, in the case of water, higher molar volume would give lower solubility. Furthermore, they describe the solubility of polar and nonpolar gases in several ILs by means of solubility parameter which is conceptually close to what Blanchard proposed. But, they failed to find a trend in the enthalpy and entropy of solvation for describing the solubility order of studied gases.[25] The same conclusion about the enthalpy and entropy of solvation can be obtained by inspecting the data reported by Jacquemin et al.[29] for solubility of different gases in $[bmim][PF_6]$. Also, Richard Noble and his co-workers successfully used regular solution theory and solubility parameters to describe and correlate solubility of nonpolar gases such as CO_2, O_2, N_2, CH_4, and C_2H_4 in mostly imidazolium-based ILs,[30−32] but nothing has been reported for polar gases such as SO_2 and water.

Huang et al.[24,33] used H NMR and Fourier transform IR (FTIR) spectra to show that SO_2 is purely physically absorbed in ILs. Also, they experimentally disclose the effect of temperature on the solubility order of SO_2 in ILs. This may motivate one to conclude that explanation of gas solubility in ILs based on molar volume could be oversimplification since molar volume is not changing significantly by temperature. Shi et al.[34] used Monte Carlo simulation to investigate the solubility of SO_2, CO_2, N_2, O_2, and some of their mixtures in IL 1-hexyl-3-methylimidazolium bis-(trifluoromethyl) sulfonylimide ($[hmim][Tf_2N]$). They showed higher solute−IL interaction can lead to higher solubility of gas in IL and the interaction between gas and anion is larger than gas−cation. Also, they demonstrated using regular solution theory for explaining gas solubility in IL comes with some limitations and is only applicable when the IL solubility parameter is fit to available experimental data. Prasad et al.[35] confirmed these results by ab initio calculations for SO_2, CO_2, and N_2 interacting with several 1,3-dimethylimidazolium ($[dmim]^+$) based ILs. The last two studies could explain why one solute is more soluble than another solute in one single IL. But, the reason behind the solubility order of one solute in different ILs is still unknown.

In this work, we used Monte Carlo simulations to find a criterion that can explain the solubility order of SO_2 and CO_2 at $P = 1$ bar in several imidazolium-based ILs. The studied ILs were $[bmim][BF_4]$, $[bmim]^+$ bromide ($[Br]^-$), $[bmim][PF_6]$, $[bmim][NO_3]$, $[bmim][Tf_2N]$, and 1-ethyl-3-methylimidazolium tetrafluoroborate ($[emim][BF_4]$). These ILs are selected to cover a wide range of cation−anion interactions from weak to strong. To make sure that all ILs are in the liquid rather than crystalline phase, the main focus is on systems at $T = 323$ K. this is crucial especially for $[bmim][Br]$ and $[bmim][NO_3]$ with melting points equal to 318 and 309 K, respectively.[36,37] For validation purposes, some pure ILs and CO_2/IL mixtures are simulated at $T = 298$ K.

2. SIMULATION DETAILS

2.1. Force Field (FF). The interaction potential models proposed by Sokolic et al.[38] and Potoff et al.[39] were used for SO_2 and CO_2 molecules, respectively. In these models, the molecule is approximated as three sites representing for each atoms. Each site is the center of a Lennard-Jones (LJ) potential with an embedded central point charge. The functional form of intermolecular potential used for SO_2 and CO_2 is presented below

$$u_{ij} = 4\varepsilon_{ij}\left(\left(\frac{\sigma_{ij}}{r_{ij}}\right)^{12} - \left(\frac{\sigma_{ij}}{r_{ij}}\right)^{6}\right) + \frac{q_i q_j e^2}{r_{ij}} \quad (1)$$

The FF used for ionic liquids is based on a united atom model and has the functional form of OPLS-UA[40] but bond length and bond angles considered to be constant. The final form is as follows

$$u_{ij} = \sum_{\text{dihedrals}} \frac{V_n}{2}[1 + (-1)^{n+1}\cos(n\varphi)] + 4\varepsilon_{ij}\left(\left(\frac{\sigma_{ij}}{r_{ij}}\right)^{12} - \left(\frac{\sigma_{ij}}{r_{ij}}\right)^{6}\right) + \frac{q_i q_j e^2}{r_{ij}} \quad (2)$$

The first term on the right-hand side is the sum over dihedral angles. Nonbonded interactions are included by second and third terms for van der Waals (VDW) and electrostatic (EL) interactions of atom-centered point charges, respectively. The nonbonded interactions are calculated for either atoms in different molecules or in the same molecule separated by at least three bonds. The nonbonded VDW interactions separated by exactly three bonds (1−4 interactions) are multiplied by $^1/_2$. Molecular parameters for studied ILs are taken from literature.[41−45] The LJ parameters for unlike atoms are obtained from the Lorentz−Berthelot combining rule, i.e., arithmetic and geometric mean rules for the cross size and energy parameters, respectively. The structures of isolated ions have been optimized by Gaussian 03.[46] It should be noted that the imidazolium ring in ILs was constrained to be planar.

2.2. Pure ILs. Monte Carlo simulations of pure ILs were performed in the isothermal−isobaric (NPT) ensemble using the Metropolis acceptance rule. The simulation package is an in-house-developed computer code, and it is validated against liquid density and total potential energy of pure ILs as described in the Results and Discussion section. Systems consisted of a total of N ions pairs in a cubic simulation box with standard periodic boundary conditions. A spherical atom-based cutoff equal to $L/2.0$ was used where L is the length of the simulation box. Initial configurations were a simple face-centered cubic lattice.

Standard long-range corrections for LJ interactions were applied. The long-range EL interactions were treated using the Wolf method.[47] The Wolf method is formally very close to the conventional Ewald summation method[48] but requires less computational time, while for homogeneous dense systems it provides almost as accurate results as Ewald summation method.[49,50] This is discussed more in section 3.2. The cutoff distance of the Wolf method was half of the simulation box length, and the convergence parameter was set to $3.7/L$.

Each run was comprised of equilibration and production periods with 10^6 cycles for every period. In a cycle, one cation and one anion were chosen by random and a package of movements consisting of displacement, rotation, and dihedral angle change (if applicable) were executed with 50% acceptance ratio. The size of the simulation box was altered after each $2N$ cycles. It should be noted that in order to obtain statistical errors four different independent runs were conducted for each system.

2.3. Gas Solubility. To calculate the solubility of a solute in ILs, an improved Widom particle insertion method[51,52] was used. On the basis of this method, the chemical potential of the solute in the isothermal−isobaric ensemble is given by[52,53]

$$\mu_s^{ex} \equiv \mu_s - \mu_s^{ideal} = -k_B T \ln\left[\frac{\langle V e^{-\beta\psi_s}\rangle}{\langle V\rangle}\right] \quad (3)$$

Where μ_s^{ex} is the difference between the actual chemical potential μ_s and the ideal gas chemical potential μ_s^{ideal} and ψ_s is the energy experienced by a "ghost" particle that interacts with the rest of the molecules. V represents the system volume and $\beta = 1/k_BT$ where k_B and T denote the Boltzmann constant and temperature, respectively. Then, the Henry's constant of the solute in the solvent, H_s, is obtained by the following expression

$$H_s = \rho RT \exp(\beta\mu_s^{\infty ex}) \quad (4)$$

where ρ is the density of the solvent and $\mu_s^{\infty,ex}$ is the infinite dilution chemical potential of solute in ILs. In the original form of this method, the solute molecule with a random orientation is randomly inserted into the simulation box, and the energy ψ_s is calculated each time. The act of ghost molecule insertion continues until the calculated excess chemical potential converges to a number.

The Widom particle insertion method is the simplest way to estimate the Henry's constant, and it is shown that it suffers from poor convergence especially in dense solvents.[54] Although, for small solutes such as CO_2 and SO_2 the convergence issue seems to be less sever. In this work, finding an index for the solubility order is the main goal rather than reproducing experimentally observed Henry's constant. So, this deficiency will not considerably affect the analysis procedure. Yet to increase the portion of accepted insertions and improve the convergence, the simulation box is divided into small cubelets. A cubelet is considered as vacant if it does not include the center of mass of any ions in the simulation. After every $2N$ cycles, all cubelets are checked to determine whether they are vacant or occupied. Then, one solute molecule with a random orientation is inserted into each unoccupied cublets at a time. Finally, the interaction energy experienced by the ghost molecule is used to calculate Henry's constant of solute in the IL. This procedure is continued until the calculated Henry's constant converges with an acceptable error bar. The number of cubelets varies from 2200 to 2700 for different ILs. The higher number of cubelets is more suitable for ILs with stronger interaction between anion and cation since in these cases the probability of finding an empty cubletes is less.

2.4. Solute/IL Mixtures. To study the interaction between solute and ILs, mixtures of N ionic pairs and 10 solute molecules were simulated. The low concentration of solute in IL phase is inevitable to minimize the solute−solute interactions and mimic the situation where $\mu_s^{\infty,ex}$ was calculated by the Widom method. Simulation details for these mixtures are almost as before, but now, in each cycle, one cation, one anion, and one solute molecule are chosen randomly and a set of molecular motions applied on each of them, consecutively. In addition, for validation purposes, a simulation with Ewald summation instead of Wolf method was conducted for one solute/IL mixture with $L/2$ and $1.9/L$ as cutoff distance and convergence factor, respectively. The equilibrium molecular configurations achieved by simulations of this section were used to compute interaction energies between solute and ions as well as radial distribution functions (RDF) for solute−IL mixtures.

Table 1. Liquid Density (ρ) of Pure ILs and SO_2/IL Mixtures at P = 1 bar[a]

IL	x^{IL}	T (K)	ρ_{sim}(g/cm^3)	ρ_{exp}(g/cm^3)	RD%
[bmim][BF_4]	1.0	298	1.213 ± 0.006	1.204[41]	0.7
		323	1.206 ± 0.004	1.188 ± 0.002[25]	1.5
SO_2/IL	0.96	323	1.202 ± 0.005		
CO_2/IL	0.96	323	1.204 ± 0.005		
[emim][BF_4]	1.0	298	1.247 ± 0.005	1.280[58]	−2.6
		323	1.235 ± 0.005	1.262[58]	−2.1
SO_2/IL	0.96	323	1.231 ± 0.004		
[bmim][Br]	1.0	323	1.321 ± 0.004	1.280[36]	3.2
SO_2/IL	0.96		1.314 ± 0.005		
[bmim][Tf_2N]	1.0	323	1.462 ± 0.006	1.44[59]	1.5
SO_2/IL	0.96		1.447 ± 0.004		
[bmim][NO_3]	1.0	323	1.233 ± 0.006	1.137[60]	8.4
				1.157[42]	6.5
SO_2/IL	0.96		1.223 ± 0.006		
CO_2/IL	0.96	323	1.223 ± 0.005		
[bmim][PF6]	1.0	298	1.382 ± 0.004	1.360 ± 0.008[61]	1.5
		323	1.371 ± 0.003	1.340 ± 0.008[61]	2.2
SO_2/IL	0.96	323	1.368 ± 0.004		

[a] x^{IL} is the mole fraction of the IL in the mixture.

Table 2. Total Intermolecular Interaction U (kJ/mol) and Its LJ and EL Contributions for Selected ILs at T = 298 K and P = 1 bar

IL	U_{sim}^{LJ}	$U_{sim}^{LJ\ 41}$	U_{sim}^{EL}	$U_{sim}^{EL\ 41}$	$U_{sim}^{tot\ 41}$
[bmim][BF_4]	−65.0 ± 0.1	−66.3	−444.1 ± 0.1	−445.2	−512.6
[emim][BF_4]	−46.6 ± 0.2	−51.9	−453.2 ± 0.2	−457.6	−509.5
[bmim][PF6]	−74.9 ± 0.1	−75.2	−419.1 ± 0.2	−423.4	−498.6

3. RESULTS AND DISCUSSION

3.1. IL Density. Liquid density is one of the common ways to validate FFs and simulation packages. In the case of RTILs, it is worthy mentioning that sometimes trace amount of impurities like water, chlorine, and sodium ions could change the density considerably.[55] So, before doing any comparison, one should have reliable experimental data. Table 1 compares liquid density of studied system at P = 1 bar with available experimental data. The average relative deviation of pure IL densities from experimental data is 2.9%, which has the same order of magnitude of similar studies published in the literature.[43,45,56]

The only concern appear to be [bmim][NO_3] system where the relative deviation is about 7% higher than experimental values. FF parameters of $[bmim]^+$, $[BF_4]^-$, and $[PF_6]^-$ are taken from Liu et al.,[41] and as it can be seen from Table 1, simulated liquid densities for [bmim][BF_4] and [bmim][PF_6] ILs are within 3% of the reported experimental data. Also, liquid density of [bmim][Br] and [bmim][Tf_2N] systems, with parameters of anion FF adopted from Lopez et al.,[43,44] deviate very slightly from available experimental data. So, we conclude that FF of the [bmim] cation is optimized in a way that it might be combined freely with any other anions, available in the literature, at a negligible risk. On the other hand, when $[NO_3]^-$ with FF reported by Lopez et al.[42] is used with [bmim] cation with FF parameters optimized by the same author (Lopez et al.[42]), the

Table 3. Contributions of Total EL Interactions Calculated by the Wolf Method and Ewald Summation for SO_2/[bmim][Br] mixture at T = 323 K and P = 1 bar

SO_2/[bmim][Br]	S−S	S−C	S−A	C−C	C−A	A−A
Wolf method	−0.001	−0.228	−0.534	658.6	−1724.2	597.6
Ewald summation	0.081	−0.224	−0.533	652.0	−1703.2	599.0
RD% = $((E^{Wolf} - E^{Ewald})/(E^{Ewald})) \times 100$	NA	−1.7	−0.2	+1.0	−1.2	−0.2

deviation of simulated liquid density from experimental data is less than 2%. But, when we combined $[NO_3]^-$ with $[bmim]^+$ taken from Liu et al.,[41] the deviation of liquid density was about 7%. Therefore, we may assume that the FF for $[NO_3]^-$, optimized by Lopez et al.,[42] just functions when it is used with cations published by the same research group. Consequently, $[NO_3]^-$ FF might need further optimization as an individual ion not a combined cation−anion molecule. Cadena et al.[57] have also addressed the issue of $[NO_3]^-$ FF, parametrized by Lopez et al.[42]

Finally, it can be seen from Table 1 that the pure IL density is at most 2% higher than the density of IL/solute mixtures. It might be explained by the "space filling mechanism," which assumes the gas molecule place in available empty spaces between anion and cation. This is consistent with what Brenneck et al.[11] found for CO_2 and contradicts with the results of Ando et al.[36] where a significant increase in the density of [bmim][Br] observed when it exposed to small amount of SO_2 gas.

3.2. Intermolecular Interactions. Table 2 compares the total intermolecular interaction and its LJ and EL contributions for some selected ILs with the corresponding values simulated by Liu et al.[41] at T = 298 K and P = 1 bar using the same FF with the same set of parameters. By average, the absolute values of LJ contribution is about 6% less than Liu et al.[41] This deviation might be attributed to the different simulation details. Liu et al.[41] have done the NPT molecular dynamic simulation using MDynaMix program[62] with N = 128 and a fixed cutoff distance equal to 1.5 nm where L was at least 3 nm. In this work, the NPT Monte Carlo simulation was conducted for N = 256 ion pairs with the cutoff distance equal to the half of the simulation box. Also they have not mentioned whether the long-rang corrections is added to LJ contribution or not while we modified the interaction energy to compensate for the missing long-range part of the potential[63] even though the cutoff radius is large enough.

The EL contribution calculated by Wolf method deviates around only 1% from the results of Liu et al.[41] computed by the standard Ewald sum method. This clearly shows that, for pure IL systems, using the less computationally expensive method of Wolf and ignoring the self-image interactions provides almost the same results as the traditional Ewald sum while the simulation run time is considerably less.

The same acceptable consistency between the Wolf method and the Ewald sum is achieved for dilute solute/IL mixtures as it is shown in Table 3 for EL intermolecular interactions (kJ/mol) of SO_2/[bmim][Br] system at T = 323 K and P = 1 bar with simulation details described in section 2.4. Error bars are in the same order as the total EL interactions presented in Table 2 and are omitted here for more clarity. The only problem seems to be the solute−solute (S−S) interaction where the Wolf method significantly underestimates the EL interaction energy. The solute molecule is at dilute concentration, and S−S has a negligible contribution to the total EL interactions. Also, as it will be discussed in section 3.4, cross interactions, namely, solute−cation (S−C), solute−anion (S−A), and cation−anion (C−A), rather than self-interactions dominate the solubility order of solutes in ILs. Consequently, neither the overall trend nor the solubility of solute is affected by this deficiency. The deficiency of truncated methods such as Wolf is inspected in more detail by Mendoza et al.[50] and Furse et al.[64] Basically, as it is examined by Furse et al.[64] and Denesyuk et al.,[65] for simple and small solute molecules in dense solvents as well as symmetric ionic fluids, it is not risky to substitute the Ewald summation with damped and cutoff-neutralized Coulombic sums such as damped shift force, local molecular field, and the Wolf method.[66]

3.3. Gas Solubility. For calculation of Henry's constant (H), as in the case of liquid density, four independent runs are used to get the uncertainty. For each run, H is estimated by the procedure described in section 2.3. Figure 1 shows the Henry's constant convergence for three different systems. It is well-known that particle insertion method suffers from convergence problems; it overestimate the solubility of gas in ILs, and also it is strongly dependent to system size.[54] But, presenting the best estimation of gas solubility in IL was not our main goal here. The relative solubility, or in other words, solubility order of solute is desirable in our analysis. To validate the computer codes used for calculation of gas solubility in ILs, we compared Henry's constant of CO_2 in $[bmim][PF_6]$ with those published by Shah et al.[54] and an acceptable agreement has been obtained. Table 4 summarizes these results together with those of SO_2 in studied ILs.

As mentioned earlier, ILs are mainly studied at T = 323 K to make sure that all ILs are in the liquid rather than the crystalline phase, which provides the opportunity to investigate ILs with strong C−A interactions such as [bmim][Br] and $[bmim][NO_3]$. Unfortunately, H of SO_2 in studied ILs at T = 323 K is not reported in the literature. Hence, for comparison, in Table 4 we presented the experimental equilibrium mole fraction of the solute in IL. As it can be seen from this table, SO_2 is quite soluble in all tested ILs and by considering the large error bars on simulated Henry's constant, the solubility order might be written as

$$[bmim][Br] \approx [bmim][NO_3] > [bmim][Tf_2N] \approx [bmim][BF_4] \approx [emim][BF_4] > [bmim][PF_6]$$

The solubility of SO_2 in $[bmim][Tf_2N]$ is predicted to be higher than $[bmim][BF_4]$, while the experimental data for SO_2 presented in Table 4 shows the following solubility order: $[bmim][Tf_2N] \approx [bmim][BF_4] > [bmim][PF_6]$.

This is almost consistent with results of Jiang et al.[21] where the mole fraction of SO_2 in some supported imidazolium-based IL membranes at T = 298 K and P = 1 bar was reported to be in a narrow range with the solubility order

$$[bmim][BF_4]\ (0.570) > [bmim][Tf_2N] \approx [emim][BF_4]\ (0.551) > [bmim][PF_6]\ (0.536)$$

The numbers in the parentheses with error bars around 0.01 are the equilibrium mole fraction of SO_2. Generally, it is interesting that SO_2 seems more soluble in ILs with smaller molar volumes.

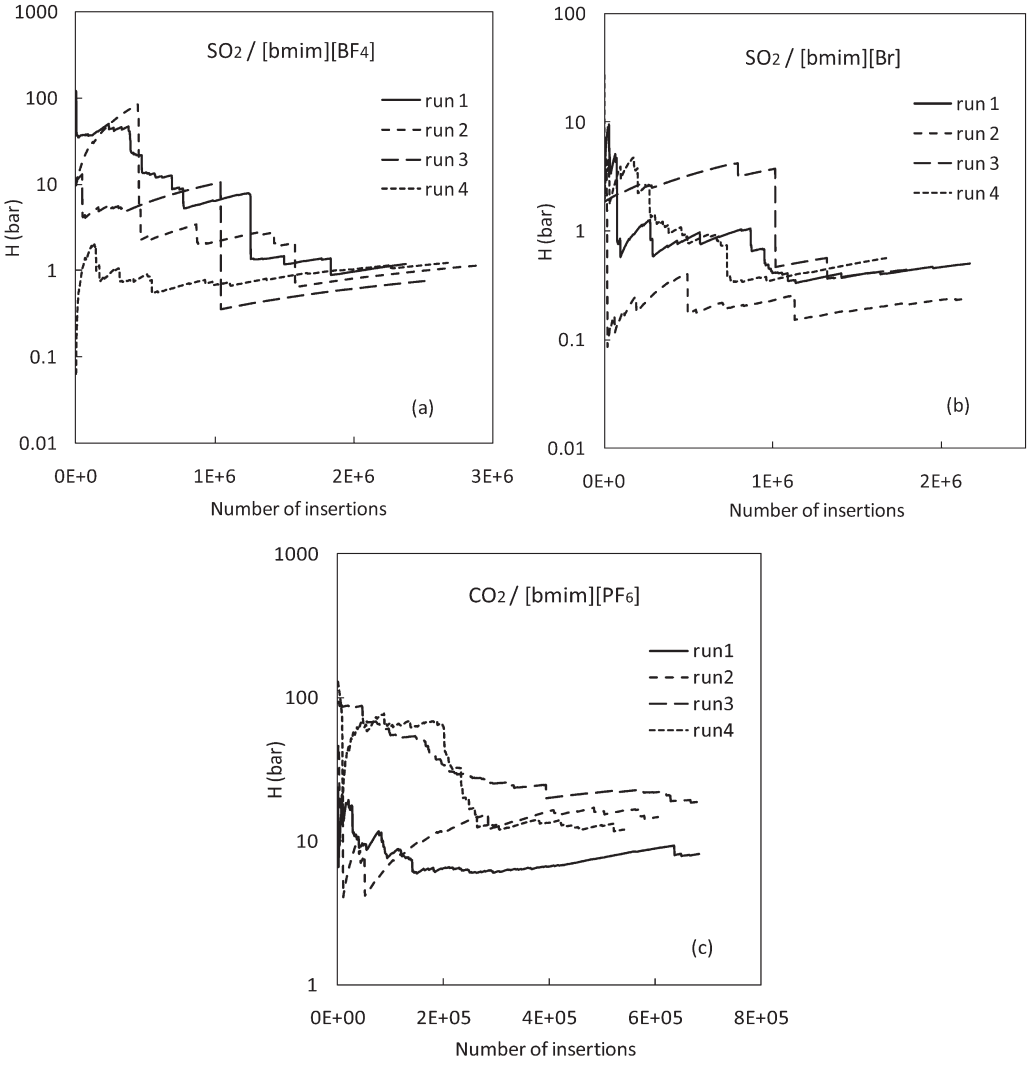

Figure 1. Convergence of Henry's constant (H). (a) SO_2 in [bmim][BF_4] and (b) SO_2 in [bmim][Br] at T = 323 K with N = 250. (c) CO_2 in [bmim][PF_6] at T = 298 K with N = 100.

Table 4. Henry's Constant (H) of SO_2 and CO_2 in Studied ILs at P = 1 bar[a]

solute	IL	T (K)	N	H_{sim} (bar) this work	H_{exp} (bar)	H_{sim} (bar)	$x^{solute,exp}$
CO_2	[bmim][PF_6]	298	100	15.5 ± 3.3	53.4 ± 0.3[67]	15 ± 5[54]	
	[bmim][PF_6]	323	250	41.9 ± 4.0	81.3 ± 0.5[67]	48 ± 6[54]	
	[bmim][BF_4]	323			88.6 ± 1.9[25]		
SO_2	[bmim][BF_4]	323	250	1.12 ± 0.23			0.32,[68] 0.38[24]
	[emim][BF_4]			1.37 ± 0.35			
	[bmim][Br]			0.44 ± 0.11			
	[bmim][Tf_2N]			0.80 ± 0.24			0.36[24]
	[bmim][NO_3]			0.43 ± 0.15			
	[bmim][PF6]			1.64 ± 0.48			0.27[68]

[a] $x^{solute,exp}$ is the experimental equilibrium mole fraction of solute in IL.

This trend resembles the behavior of water in ILs while molecules like N_2, CO_2, and O_2 are more soluble in ILs with lower molar volume.[25,28] On the other hand, enthalpy and entropy of solvation can be considered to predict the solubility order of different solutes in a IL, but they are unable to describe the solubility order of one solute in different ILs.[25,34,35] In addition, the solubility order of a solute in various ILs changes by temperature,[24,33] while molar volume of ILs is a weak function of temperature. As mentioned earlier, these observations reveal the complex nature of solute/IL mixtures. The simulation of IL/solute mixtures can provide a valuable understanding of this complicated trend by disclosing specific information about C—A,

dx.doi.org/10.1021/jp2051239 |J. Phys. Chem. B 2011, 115, 13599–13607

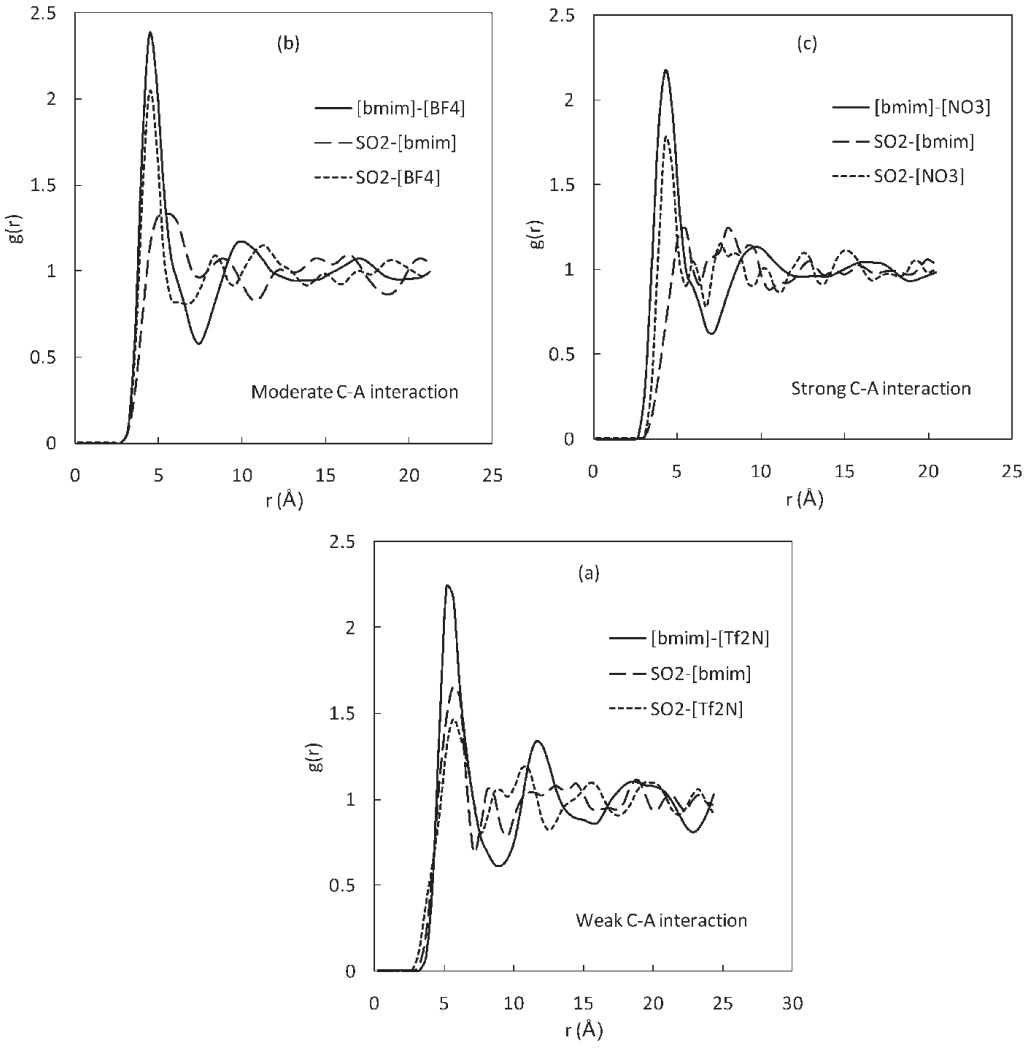

Figure 2. Center of mass−center of mass RDF for SO_2/ILs mixtures at $T = 323$ K and $P = 1$ bar. [bmim][Tf_2N], [bmim][BF_4], and [bmim][NO_3] are considered as representatives of weak, moderate, and strong C−A interactions, respectively.

S−A, and S−C interactions that may lead to a reason for solubility order of gases in ILs.

3.4. Gas−IL Mixtures. The relative height of the first pick of RDF computed for interaction between different components of a mixture might be a valuable index to investigate the microstructure of a system. Figure 2 presents center of mass−center of mass RDF for SO_2 in [bmim][Tf_2N], [bmim][BF_4], and [bmim][NO_3] at $T = 323$ K and $P = 1$ bar. Interaction between anion and cation in these ILs can be assumed as weak, moderate, and strong, respectively, which is based on calculated C−A interaction energies, and it will be discussed later in this section. This sheds light on how the interaction between cation and anion can affect the gas solubility.

As one can expect, the S−A interaction is greater when the charge density on anion molecule is higher. For instance, in the case of [bmim][NO_3], it is even comparable with C-A interaction. But, it is interesting that the order of S−A interaction is not the same as the solubility order of SO_2 in these ILs. Also, as it can be interpreted from this figure, S−C interaction decreases when the S−A interaction increases. So, even for ionic liquids with the same cation, the S−C interaction is affected by the S−A interaction.

Figure 3 characterizes the site−site RDFs for SO_2/[bmim]-[BF_4] and SO_2/[bmim][NO_3] mixtures and Figure 4 shows the atomic label scheme for $[bmim]^+$ cation. In addition to a strong S−A interaction, there are three distinguishable active sites on the cation, H4, H5, and alkyl chain connected to atom N of the imidazolium ring for attracting the solute molecule. It would be worthy to mention that there is a competition between anion and solute over H5 site. The tendency of anion to locate around H5 site has been pointed out by several authors.[35,69−72] So, as it can be seen from Figure 3, a stronger C−A interaction pushes the solute toward H4 site leading to a sharper S−H4 peak.

These observations together with those obtained from Figure 2 prove that, in order to understand the gas solubility in ILs, S−C interactions must be considered as well as the contributions of S−A and C−A interactions. This would be straightforward to conclude that stronger solute−IL interaction (S−IL = S−C + S−A) can result in higher solubility of solute in IL. One can relate the total interaction of a solute with IL ions to enthalpy of solvation, but the enthalpy of solvation by itself cannot describe the solubility order of gases in ILs.[25,29] On the other hand, since the solute is dissolved in IL according to space filling mechanism,[11] the solubility of gas in an IL with bulkier ions is more.[25,29]

dx.doi.org/10.1021/jp2051239 |J. Phys. Chem. B 2011, 115, 13599–13607

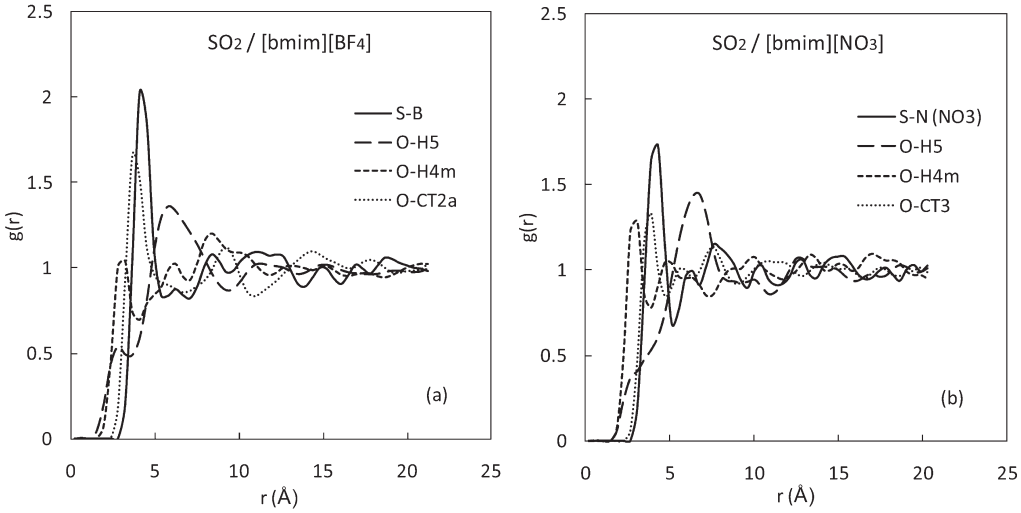

Figure 3. Site−site RDF for SO_2 and IL interactions at T = 323 K and P = 1 bar.

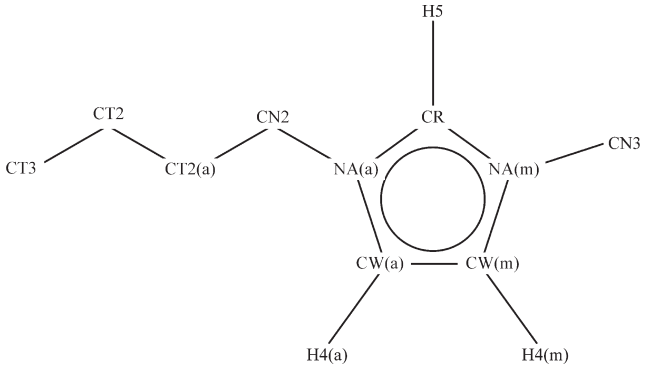

Figure 4. Atomic label scheme for $[bmim]^+$ cation.

This solubility index proposed by Anthony et al.[25] and Blanchard et al.[27] can describe the solubility order of nonpolar molecules such as O_2, N_2, C_2H_4, and CO_2, but it fails to explain the solubility order of water and SO_2. So, each of these criteria is unable to duplicate the solubility order of different types of solutes in ILs. But, a combination of both might be a suitable index to serve this purpose.

3.5. Solubility Index. Therefore, a new solubility index (ξ) is introduced in this work as the ratio of the S−IL interaction and C−A interaction energy density which is a mathematical combination of the two criterions mentioned earlier

$$\xi = \frac{(\mathrm{S}-\mathrm{IL})}{[(\mathrm{C}-\mathrm{A})\times\rho]^{1/3}}[=]\frac{kj^{2/3}\mathrm{cm}}{\mathrm{mol}} \qquad (5)$$

where C−A is the ensemble average of cation−anion intermolecular interactions for pure IL, S−IL is the sum of the ensemble averages of solute−cation and solute−anion intermolecular interactions in solute/IL mixtures, and ρ is molar density of mixture. When the S−IL interaction is larger, the solubility is expected to be higher. Higher S-IL interaction increases the nominator of eq 5 leading to larger ξ and higher solubility. On the other hand, when the IL has bulkier ions, the molar density is smaller and also ions carry less charge density which causes weaker C−A interaction. So, the denominator of eq 5 would be smaller, which results in higher ξ and higher solubility of solute based on the concept of solubility parameter. Consequently, the larger the index ξ for a solute in IL, the higher the solubility.

Table 5 summarizes various contributions of the SO_2 and CO_2 interaction energies with studied ILs along with the solubility index (ξ) proposed in this work shown in bold. The uncertainty of reported values has the same order of magnitude for all studied systems and it is shown just for SO_2/[bmim][Br] mixture. As it can be seen from Table 5, for all cross interactions when ions are bulkier, like the case of [bmim][Tf_2N], the LJ contribution is larger while EL contribution is smaller. Inspecting different contributions of interaction energies between solute and ILs demonstrate that they cannot explain the solubility order of SO_2 and CO_2 in studied ILs. But, based on the values of ξ, the solubility order of CO_2 in studied ILs is as follows

$$[bmim][PF_6] > [bmim][BF_4] > [bmim][NO_3]$$

This perfectly matches the experimental solubility order of CO_2 in these ILs published by Anthony et al.[25] and Blanchard et al.[27] In the case of CO_2, the solubility index of these authors presented in the last row of Table 5, which is conceptually close to the solubility parameter (δ), can also describe the solubility order. On the other hand, this index leads to nonsense results for solubility of SO_2 in ILs. While ξ is in satisfying agreement with the simulation results of this work shown in Table 4 and also with the experimental data of Jiang et al.,[21] Huang et al.[24] and Lee et al.[68] discussed earlier in this section. Also, it should be noted that the ξ of SO_2 is generally higher than the corresponding values for CO_2, which again is consistent with the available experimental data. The only issue seems to be the value of ξ for SO_2/[bmim][NO_3], which based on the results of Table 4 and the discussion ascribed to that, expected to be closer to ξ of SO_2/[bmim][Br] rather than SO_2/[bmim][BF_4]. This can be attributed to the problem described in section 3.1 regarding the FF parameters of $[NO_3]^-$.

It is important to mention that having bulkier ions is equivalent to less molar density. So, when the pure molar density of the IL is, for example, overestimated, then the C−A interaction is overestimated. But, this can affect the environment that the "ghost" particle experience, and consequently the S−IL interaction might be either underestimated or overestimated. Therefore, it would be burdensome to predict how ξ is affected by

dx.doi.org/10.1021/jp2051239 |J. Phys. Chem. B 2011, 115, 13599–13607

Table 5. EL and LJ Contributions of C−A, S−A, Solute−IL, and C−A Interactions (kJ/mol) at T = 323 K and P = 1 bar[a]

	SO_2 solute						CO_2 solute		
IL	[bmim] [Br]	[bmim] [NO_3]	[bmim] [BF_4]	[bmim] [Tf_2N]	[emim] [BF_4]	[bmim] [PF_6]	[bmim] [PF_6]	[bmim] [BF_4]	[bmim] [NO_3]
S−C EL	−0.228	−0.218	−0.331	−0.264	−0.440	−0.214	−0.416	−0.321	−0.315
S−C LJ	−1.173	−1.171	−1.063	−0.770	−0.963	−0.780	−0.661	−0.767	−0.812
S−C tot	−1.401	−1.389	−1.394	−1.034	−1.403	−0.994	−1.077	−1.088	−1.127
S−A EL	−0.534	−0.568	−0.339	−0.056	−0.315	−0.323	−0.279	−0.275	−0.121
S−A LJ	−0.677	−0.220	−0.312	−0.627	−0.285	−0.346	−0.142	−0.164	−0.194
S−A tot	−1.211	−0.788	−0.651	−0.683	−0.600	−0.669	−0.421	−0.439	−0.315
S−IL	−2.612	−2.177	−2.045	−1.717	−2.003	−1.663	−1.498	−1.527	−1.442
C−A EL	−1724	−1752	−1661	−1488	−1689	−1612	−1612	−1661	−1752
C−A LJ	2.329	−22.03	−20.5	−75.19	−15.61	−35.29	−35.29	−20.5	−22.03
C−A tot	−1722	−1773.6	−1681	−1563	−1705	−1647	−1647	−1681	−1773.6
ξ	**0.945**	**0.784**	**0.781**	**0.774**	**0.723**	**0.661**	**0.596**	**0.583**	**0.519**
$\delta \propto (1/\rho)$	81.6	82.9	93.6	143.5	80.1	103.6	103.6	93.6	82.9

[a] New solubility index (ξ) in comparison with solubility parameter (δ[=]cm^3/mol) proposed by Anthony et al.[25] and Blanchard et al.[27] Error bars are less than 2% for solute−IL and less than 1% for C−A interactions.

calculated bulk molar density. Also, it should be noted that the S−IL interaction is calculated for a mixture of 250 ionic pairs and just 10 solute molecules. This is inevitable when one is dealing with Henry's constant since it is computed by the chemical potential at infinite dilution of solute in ILs. When the concentration of solute in IL phase is not small then the solute−solute interactions and the effect of solute on C−A interactions cannot be simply ignored. For these cases, more investigation is needed and the above analysis would not be valid anymore.

In general, the proposed solubility index appears to be promising in matching the solubility orders of SO_2 and CO_2. Although, we chose SO_2 and CO_2 as representatives of polar and nonpolar solutes, respectively, the validity of ξ needs to be examined against other gases as well as other types of ILs. When the applicability of this solubility index is approved, it could be used as an alternative to time-consuming methods of Henry's constant calculations when just the solubility order is preferred.

CONCLUSION

The solubility of SO_2 and CO_2 at P = 1 bar in different imidazolium-based ILs is calculated using NPT Monte Carlo simulation and the Widom particle insertion method. Furthermore, to understand the interaction between solute and ILs and also to find a solubility index for polar and nonpolar gases in ILs, solute/IL mixtures have been simulated with the mole fraction of solute around 0.04. The results show that neither solute−IL interactions nor molar volume of ILs can describe the solubility order of SO_2 and CO_2 when they are used separately. Also, it is revealed that, to some extent, S−C interactions might be as important as S−A interactions for both polar and nonpolar solutes. On the basis of these observations, the ratio of S−IL interaction and C−A interaction energy density (ξ) is proposed as a solubility index for gases in IL. Comparison between ξ and simulated and experimental solubility data shows that the application of ξ in prediction of solubility orders seems promising. But, the validity of ξ for other gases and different types of ILs must be evaluated. The application of an approved ξ index can be considerably advantageous compared to standard methods of Henry's constant calculations when the solubility order is needed.

AUTHOR INFORMATION

Corresponding Author

*Phone: +1 330 972 7253. E-mail: elliot1@uakron.edu.

REFERENCES

(1) Earle, M.; Seddon, K. *Pure Appl. Chem.* **2000**, *72*, 1391.
(2) Wasserscheid, P.; Welton, T.; Corporation, E. *Ionic liquids in synthesis*; Wiley Online Library, 2003; Vol. 2.
(3) Earle, M.; Esperança, J.; Gilea, M.; Lopes, J.; Rebelo, L.; Magee, J.; Seddon, K.; Widegren, J. *Nature* **2006**, *439*, 831.
(4) Welton, T. *Chem. Rev.* **1999**, *99*, 2071.
(5) Chiappe, C.; Pieraccini, D. *J. Phys. Org. Chem.* **2005**, *18*, 275.
(6) Ross, J.; Xiao, J. *Green Chem.* **2002**, *4*, 129.
(7) Buzzeo, M.; Evans, R.; Compton, R. *ChemPhysChem* **2004**, *5*, 1106.
(8) Dyson, P. *Trans. Metal Chem.* **2002**, *27*, 353.
(9) Sheldon, R.; Lau, R.; Sorgedrager, M.; Rantwijk, F.; Seddon, K. *Green Chem.* **2002**, *4*, 147.
(10) Jain, N.; Kumar, A.; Chauhan, S.; Chauhan, S. *Tetrahedron* **2005**, *61*, 1015.
(11) Brennecke, J.; Maginn, E. *AIChE J.* **2001**, *47*, 2384.
(12) Anthony, J.; Aki, S.; Maginn, E.; Brennecke, J. *Int. J. Enrivon. Technol. Manage.* **2004**, *4*, 105.
(13) Huddleston, J.; Rogers, R. *Chem. Commun.* **1998**, *1998*, 1765.
(14) Zhao, H.; Xia, S.; Ma, P. *J. Chem. Technol. Biotechnol.* **2005**, *80*, 1089.
(15) Wu, W.; Han, B.; Gao, H.; Liu, Z.; Jiang, T.; Huang, J. *Angew. Chem., Int. Ed.* **2004**, *43*, 2415.
(16) Bates, E.; Mayton, R.; Ntai, I.; Davis, J., Jr. *J. Am. Chem. Soc.* **2002**, *124*, 926.
(17) Al-Enezi, G.; Ettouney, H.; El-Dessouky, H.; Fawzi, N. *Ind. Eng. Chem. Res.* **2001**, *40*, 1434.
(18) Philip, L.; Deshusses, M. *Environ. Sci. Technol.* **2003**, *37*, 1978.
(19) Anderson, J.; Dixon, J.; Maginn, E.; Brennecke, J. *J. Phys. Chem. B* **2006**, *110*, 15059.
(20) Yuan, X.; Zhang, S.; Lu, X. *J. Chem. Eng. Data* **2007**, *52*, 596.
(21) Jiang, Y.; Zhou, Z.; Jiao, Z.; Li, L.; Wu, Y.; Zhang, Z. *J. Phys. Chem. B* **2007**, *111*, 5058.
(22) Wang, Y.; Pan, H.; Li, H.; Wang, C. *J. Phys. Chem. B* **2007**, *111*, 10461.

(23) Shiflett, M.; Yokozeki, A. *Ind. Eng. Chem. Res.* **2009**, *49*, 1370.
(24) Huang, J.; Riisager, A.; Wasserscheid, P.; Fehrmann, R. *Chem. Commun.* **2006**, *2006*, 4027.
(25) Anthony, J.; Anderson, J.; Maginn, E.; Brennecke, J. *J. Phys. Chem. B* **2005**, *109*, 6366.
(26) Anderson, J.; Dixon, J.; Brennecke, J. *Acc. Chem. Res.* **2007**, *40*, 1208.
(27) Blanchard, L.; Gu, Z.; Brennecke, J. *J. Phys. Chem. B* **2001**, *105*, 2437.
(28) Anthony, J.; Maginn, E.; Brennecke, J. *J. Phys. Chem. B* **2001**, *105*, 10942.
(29) Jacquemin, J.; Husson, P.; Majer, V.; Gomes, M. *Fluid Phase Equilib.* **2006**, *240*, 87.
(30) Camper, D.; Scovazzo, P.; Koval, C.; Noble, R. *Ind. Eng. Chem. Res.* **2004**, *43*, 3049.
(31) Scovazzo, P.; Camper, D.; Kieft, J.; Poshusta, J.; Koval, C.; Noble, R. *Ind. Eng. Chem. Res.* **2004**, *43*, 6855.
(32) Bara, J. E.; Carlisle, T. K.; Gabriel, C. J.; Camper, D.; Finotello, A.; Gin, D. L.; Noble, R. D. *Ind. Eng. Chem. Res.* **2009**, *48*, 2739.
(33) Huang, J.; Riisager, A.; Berg, R.; Fehrmann, R. *J. Mol. Catal A: Chem.* **2008**, *279*, 170.
(34) Shi, W.; Maginn, E. *J. Phys. Chem. B* **2008**, *112*, 2045.
(35) Prasad, B.; Senapati, S. *J. Phys. Chem. B* **2009**, *113*, 4739.
(36) Ando, R.; Siqueira, L.; Bazito, F.; Torresi, R.; Santos, P. *J. Phys. Chem. B* **2007**, *111*, 8717.
(37) Strechan, A.; Kabo, A.; Paulechka, Y.; Blokhin, A.; Kabo, G.; Shaplov, A.; Lozinskaya, E. *Thermochim. Acta* **2008**, *474*, 25.
(38) Sokolic, F.; Guissani, Y.; Guillot, B. *J. Phys. Chem.* **1985**, *89*, 3023.
(39) Potoff, J.; Siepmann, J. *AIChE J.* **2001**, *47*, 1676.
(40) Jorgensen, W.; Maxwell, D.; Tirado-Rives, J. *J. Am. Chem. Soc.* **1996**, *118*, 11225.
(41) Liu, Z.; Wu, X.; Wang, W. *Phys. Chem. Chem. Phys.* **2006**, *8*, 1096.
(42) Lopes, J.; Deschamps, J.; Pádua, A. *J. Phys. Chem. B* **2004**, *108*, 2038.
(43) Lopes, J.; Pádua, A. *J. Phys. Chem. B* **2004**, *108*, 16893.
(44) Lopes, J.; Pádua, A. *J. Phys. Chem. B* **2006**, *110*, 19586.
(45) de Andrade, J.; Boes, E.; Stassen, H. *J. Phys. Chem. B* **2002**, *106*, 13344.
(46) Frisch, M. J.; Trucks, G. W.; Schlegel, H. B.; Scuseria, G. E.; Robb, M. A.; Cheeseman, J. R.; Montgomery, J. A., Jr.; Vreven, T.; Kudin, K. N.; Burant, J. C.; Millam, J. M.; Iyengar, S. S.; Tomasi, J.; Barone, V.; Mennucci, B.; Cossi, M.; Scalmani, G.; Rega, N.; Petersson, G. A.; Nakatsuji, H.; Hada, M.; Ehara, M.; Toyota, K.; Fukuda, R.; Hasegawa, J.; Ishida, M.; Nakajima, T.; Honda, Y.; Kitao, O.; Nakai, H.; Klene, M.; Li, X.; Knox, J. E.; Hratchian, H. P.; Cross, J. B.; Bakken, V.; Adamo, C.; Jaramillo, J.; Gomperts, R.; Stratmann, R. E.; Yazyev, O.; Austin, A. J.; Cammi, R.; Pomelli, C.; Ochterski, J. W.; Ayala, P. Y.; Morokuma, K.; Voth, G. A.; Salvador, P.; Dannenberg, J. J.; Zakrzewski, V. G.; Dapprich, S.; Daniels, A. D.; Strain, M. C.; Farkas, O.; Malick, D. K.; Rabuck, A. D.; Raghavachari, K.; Foresman, J. B.; Ortiz, J. V.; Cui, Q.; Baboul, A. G.; Clifford, S.; Cioslowski, J.; Stefanov, B. B.; Liu, G.; Liashenko, A.; Piskorz, P.; Komaromi, I.; Martin, R. L.; Fox, D. J.; Keith, T.; Al-Laham, M. A.; Peng, C. Y.; Nanayakkara, A.; Challacombe, M.; Gill, P. M. W.; Johnson, B.; Chen, W.; Wong, M. W.; Gonzalez, C.; Pople, J. A. *Gaussian 03*; Gaussian, Inc.: Wallingford, CT, 2004.
(47) Wolf, D.; Keblinski, P.; Phillpot, S.; Eggebrecht, J. *J. Chem. Phys.* **1999**, *110*, 8254.
(48) Ewald, P. P. *Ann. Phys.* **1921**, *369*, 253.
(49) Karasawa, N.; Goddard, W. A., III. *J. Phys. Chem.* **1989**, *93*, 7320.
(50) Mendoza, F. N.; López-Lemus, J.; Chapela, G. A.; Alejandre, J. *J. Chem. Phys.* **2008**, *129*, 024706.
(51) Widom, B. *J. Chem. Phys.* **1963**, *39*, 2808.
(52) Shing, K.; Chung, S. *J. Phys. Chem.* **1987**, *91*, 1674.
(53) Smit, B.; Frenkel, D. *Mol. Phys.* **1989**, *68*, 951.
(54) Shah, J.; Maginn, E. *J. Phys. Chem. B* **2005**, *109*, 10395.
(55) Wang, J.; Tian, Y.; Zhao, Y.; Zhuo, K. *Green Chem.* **2003**, *5*, 618.
(56) Liu, Z.; Huang, S.; Wang, W. *J. Phys. Chem. B* **2004**, *108*, 12978.
(57) Cadena, C.; Maginn, E. J. *J. Phys. Chem. B* **2006**, *110*, 18026.
(58) Curras, M.; Costa Gomes, M.; Husson, P.; Padua, A.; Garcia, J. *J. Chem. Eng. Data* **2010**, *55*, 5504.
(59) Krummen, M.; Wasserscheid, P.; Gmehling, J. *J. Chem. Eng. Data* **2002**, *47*, 1411.
(60) Seddon, K.; Stark, A.; Torres, M. *ACS Symp. Ser.* **2002**, *819*, 34.
(61) Gu, Z.; Brennecke, J. *J. Chem. Eng. Data* **2002**, *47*, 339.
(62) Lyubartsev, A. P.; Laaksonen, A. *Comp. Phys. Commun.* **2000**, *128*, 565.
(63) Allen, M. P.; Tildesley, D. J. *Computer simulation of liquids*; Clarendon Press, 1999.
(64) Furse, K. E.; Corcelli, S. A. *J. Chem. Theory Comput.* **2009**, *5*, 1959.
(65) Denesyuk, N. A.; Weeks, J. D. *J. Chem. Phys.* **2008**, *128*, 124109.
(66) Fennell, C. J.; Gezelter, J. D. *J. Chem. Phys.* **2006**, *124*, 234104.
(67) Anthony, J.; Maginn, E.; Brennecke, J. *J. Phys. Chem. B* **2002**, *106*, 7315.
(68) Lee, K.; Gong, G.; Song, K.; Kim, H.; Jung, K.; Kim, C. *Int. J. Hydrogen Energy* **2008**, *33*, 6031.
(69) Del Pópolo, M.; Lynden-Bell, R.; Kohanoff, J. *J. Phys. Chem. B* **2005**, *109*, 5895.
(70) Shah, J.; Maginn, E. *Fluid Phase Equilib.* **2004**, *222*, 195.
(71) Lee, S.; Jung, J.; Han, Y. *Chem. Phys. Lett.* **2005**, *406*, 332.
(72) Qiao, B.; Krekeler, C.; Berger, R.; Delle Site, L.; Holm, C. *J. Phys. Chem. B* **2008**, *112*, 1743.